



# **SU(3) calorons and their constituents**

E.-M. Ilgenfritz, M. Müller-Preussker and D. Peschka

Humboldt Universität zu Berlin, Germany

in collaboration with

---

B. V. Martemyanov, A. I. Veselov (ITEP Moscow)

C. Gatteringer, S. Solbrig (University of Regensburg)

P. van Baal, F. Bruckmann, D. Negradi (Univ. Leiden)

Lattice 2004, Fermilab, June 24, 2004

# Overview

- Introduction
- Generalities on  $SU(3)$  calorons
- Lattice examples
- Properties of cooled ensembles
- Summary & outlook

Recent papers:

C. Gattringer, E.-M. I., B. V. Martemyanov, M. Müller-Preussker,  
D. Peschka, R. Pullirsch, S. Schaefer, A. Schäfer,  
hep-lat/0309106, Nucl. Phys. Proc. Suppl. 129-130, 653 (2004)

E.-M. I., B. V. Martemyanov, M. Müller-Preussker, A. I. Veselov,  
hep-lat/0402010, Phys. Rev. D 69, 114505 (2004)

D. Peschka, Diploma thesis, Humboldt University (2004)

# Introduction

- Is there a relation between topology and confinement ?

As for the instanton liquid model, obviously not :

no string tension, violation of Casimir scaling;

see, however, J. Negele's talk

- What other d.o.f. might be important ?

Kovacs: both instantons and holonomies must be extracted from lattice in order to reconstruct hadronic correlators

- Who needs fractional instantons (instanton "quarks") ?

1.  $2D$   $\sigma$ -model (Fateev, Frolov, Schwarz),

2. instantons  $\rightarrow$  merons in YM (Callan, Dashen, Gross),

3. instanton melting in  $CP^{N-1}$  model (Diakonov et al.)

4. in  $\mathcal{N} = 1$  Susy YM : gluino condensation/confinement by fractional instantons (Davies et al. [1999]; Diakonov and Petrov [2003])

- Are fractional instanton solutions known ?

No. Only as constituents of finite  $T$  instantons:

calorons with non-trivial holonomy, generically composed of monopoles (dyons) of size  $1/(\pi T)$

KvBLL solutions, due to T. C. Kraan and P. van Baal (1998),  
K. Lee and C. Lu (1998)

The holonomy (Polyakov loop) determines the distribution of action (topological charge) among constituents.

- Can dissociating calorons cause the onset of confinement ?

A gas of dyons reacting to the background Polyakov loop (order parameter) would do it.

(Diakonov, Prog. Part. Nucl. Phys. 51, p. 173 [2003])

Certainly beyond semiclassics !

- To what extent can calorons be semiclassically dealt with ?

Diakonov et al. (hep-th/0404042) have semiclassically shown:

$SU(2)$  calorons become unstable w.r.t. decay into dyons at  $T_{dec}$

## What to do on the lattice ?

- Study properties of **classical solutions** in finite volume, (varying  $L_t/L_s$ ), overlap effects of constituents (with and without twist) :  
increasing overlap  $\rightarrow$  nonstatic solutions  
paper with P. van Baal, F. Bruckmann and B. Martemyanov in preparation (for  $SU(2)$ ), **talk by F. Bruckmann**  
Work done at HU Berlin mostly for  $SU(3)$  solutions.
- A **dynamical caloron mechanism** at the confinement transition ?
  1. Suggestive support for this picture by Gattringer and Schaefer (for equilibrium configurations) :  
the fermionic zero mode for  $Q = \pm 1$  configurations is found either **pinned down in deconfinement** or **jumping with changing b.c. ( $\zeta$ ) in confinement**.  
Jumping and localization of the zero mode follow the caloron-type pattern.

APE smearing : topological density supports the zero mode for all  $\zeta$ . Dyonic interpretation so far not conclusive.

2. We propose in the result of study of  $SU(3)$  calorons and equilibrium configurations :  
look for the magnetic charge content of topological clusters in the temperature range around the deconfinement transition, in this way identifying clusters as dissociated/nondissociated calorons  
(paper for  $SU(2)$  in preparation, with B. Martemyanov)

# Generalities on $SU(3)$ calorons

A simple formula for the  $SU(n)$  caloron's action ( $= \pm$  topological) density :

$$\text{Tr } F_{\alpha\beta}^2(x) = \partial_\alpha^2 \partial_\beta^2 \log \psi(x), \quad \psi(x) = \frac{1}{2} \text{tr}(\mathcal{A}_n \cdots \mathcal{A}_1) - \cos(2\pi t)$$

$$\mathcal{A}_m = \frac{1}{r_m} \begin{pmatrix} r_m & |\vec{\rho}_{m+1}| \\ 0 & r_{m+1} \end{pmatrix} \begin{pmatrix} \cosh(2\pi\nu_m r_m) & \sinh(2\pi\nu_m r_m) \\ \sinh(2\pi\nu_m r_m) & \cosh(2\pi\nu_m r_m) \end{pmatrix}$$

with

$$r_m = |\vec{x} - \vec{y}_m|, \quad \vec{\rho}_m = \vec{y}_m - \vec{y}_{m-1}, \quad \nu_m = \mu_m - \mu_{m-1}$$

here

$$b = 1/T = 1$$



## Ingredients

Asymptotic holonomy :

$$\mathcal{P}_{\infty}^0 = \text{diag} \left( e^{2\pi i \mu_m} \right), \quad \sum_{m=1}^n \mu_m = 0$$

Eigenvalues ordered as

$$\mu_1 < \mu_2 < \dots < \mu_n < \mu_{n+1} = 1 + \mu_1$$

Positions of constituents monopoles :

$$\vec{y}_1, \vec{y}_2, \dots, \vec{y}_n$$

Actions (topological charges) of constituent monopoles :

$$S_m = \nu_m S_{inst}$$

Fermion zero mode according to Atiyah-Singer index theorem,  
endowed with ad-hoc varied periodicity :

$$\Psi_{\zeta}(t + b, \vec{x}) = e^{2\pi i \zeta} \Psi_{\zeta}(t, \vec{x})$$

Jumping and delocalization of zero mode :

if  $\zeta \in [\mu_m, \mu_{m+1}] \rightarrow |\Psi_{\zeta}(x)|^2$  localized at  $\vec{y}_m$

if  $\zeta \approx \mu_m \rightarrow |\Psi_{\zeta}(x)|^2$  becomes delocalized

Interior structure of the Polyakov loop :

Holonomies at the constituents' positions  $\vec{z}_m$  (for  $SU(3)$ )

$$\mathcal{P}(\vec{z}_1) = \text{diag} \left( e^{-\pi i \mu_3}, e^{-\pi i \mu_3}, e^{2\pi i \mu_3} \right)$$

$$\mathcal{P}(\vec{z}_2) = \text{diag} \left( e^{2\pi i \mu_1}, e^{-\pi i \mu_1}, e^{-\pi i \mu_1} \right)$$

$$\mathcal{P}(\vec{z}_3) = \text{diag} \left( -e^{-\pi i \mu_2}, e^{2\pi i \mu_2}, -e^{-\pi i \mu_2} \right)$$

For well-separated constituents : all  $\vec{z}_m \rightarrow \vec{y}_m$ .

## Questions :

- How good is this realized on a lattice, i.e. in a finite volume ?
- What can we learn about solutions of higher topological charge ?

# Lattice examples

Configurations are characterized, besides by action  $S = N \frac{8\pi^2}{g^2}$  and topological charge  $Q = \pm N$ , by

- landscape in holonomy space (asymptotic and interior holonomy)
- correlation (locally) between action density and holonomy
- separation of constituents in space
- (related to) staticity

## Cooling

All studied solutions have been obtained by cooling from Monte Carlo samples in confinement, applying stopping criteria triggering on

- minimal violation of equations of motion
- maximal staticity

actually with constraints on violation of [anti-]selfduality

$$\delta_F = \sum_x \left| F_{\mu\nu}^a(x) F_{\mu\nu}^a(x) - \left| F_{\mu\nu}^a(x) \tilde{F}_{\mu\nu}^a(x) \right| \right| / S$$

A  $Q = 1$  caloron on a  $20^3 \times 4$  lattice

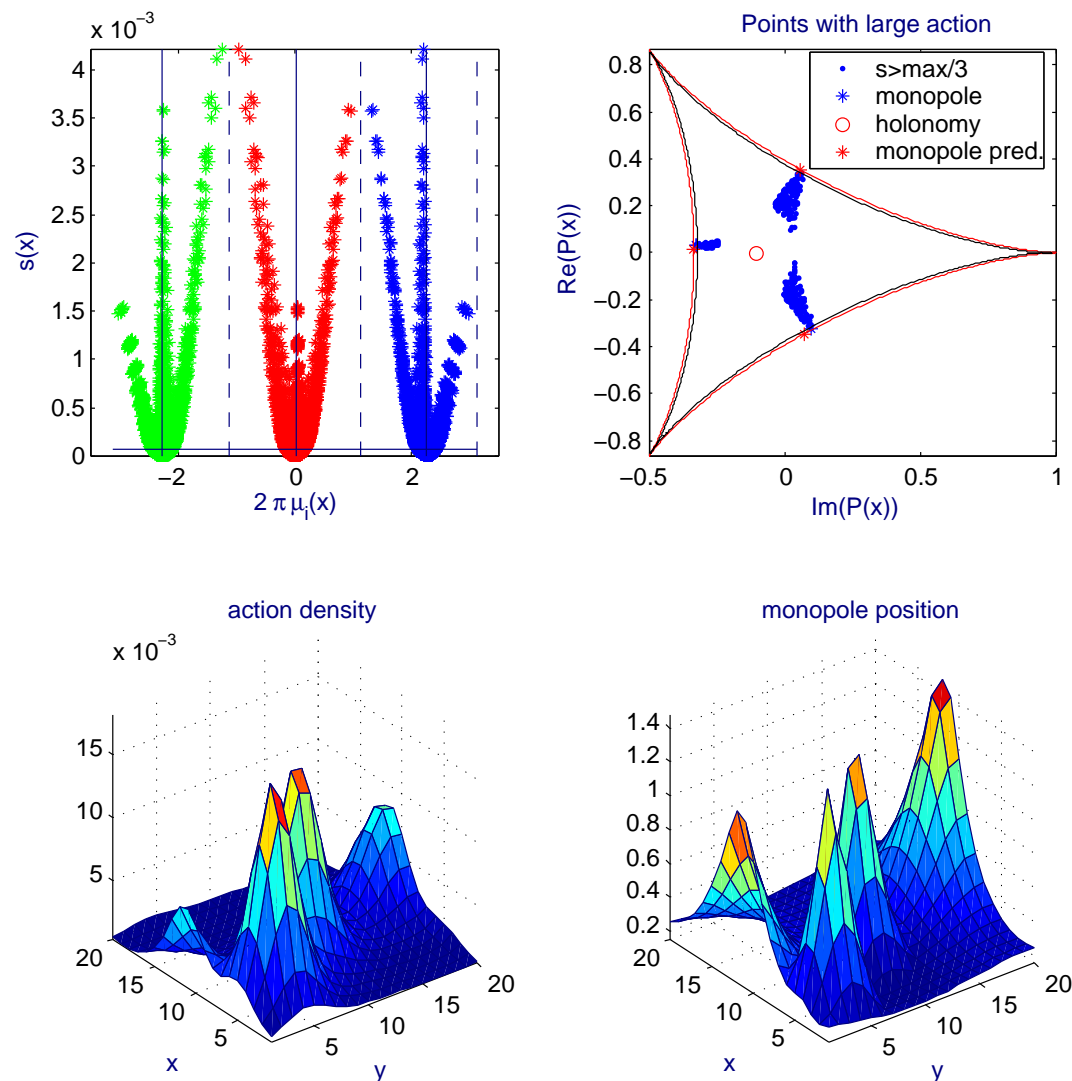


Figure 1: Holonomy eigenphases vs. action density (upper left), Polyakov loop scatter plot (upper right), action density (bottom left) and magnetic monopoles (bottom right).

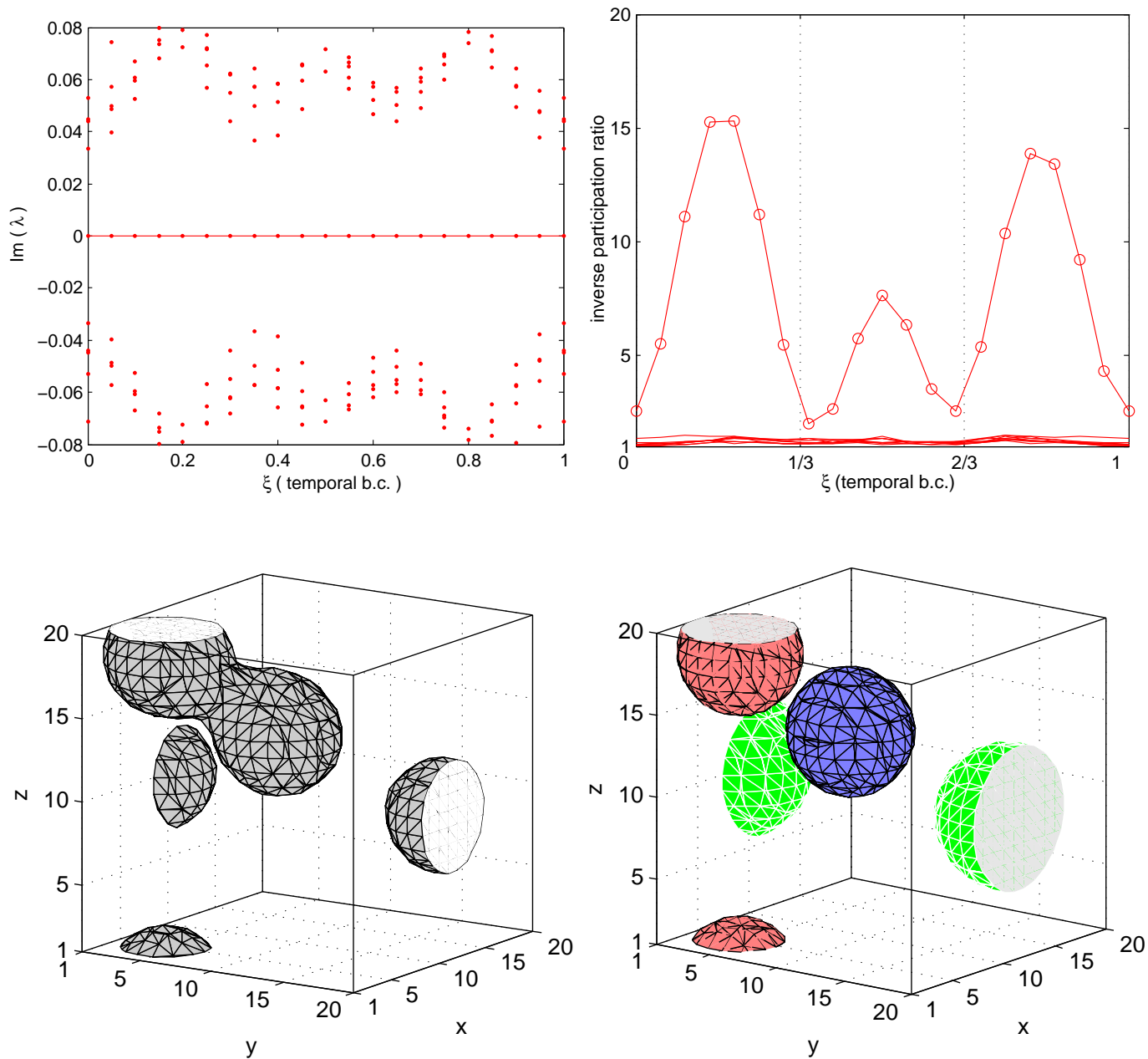


Figure 2:  $Q = 1$  caloron on  $20^3 \times 4$  : Spectral flow (upper left), inverse participation ratio (upper right), action density (bottom left) and zeromodes (bottom right) with  $\zeta$  corr. to maximal localization.

# Zero mode jumping in a static $|Q| = 1$ caloron on $12^3 \times 4$ :

cfg 092 phase 01 mode 1/1 with txyz=04 10 10 03

cfg 092 phase 04 mode 1/1 with txyz=04 07 05 03

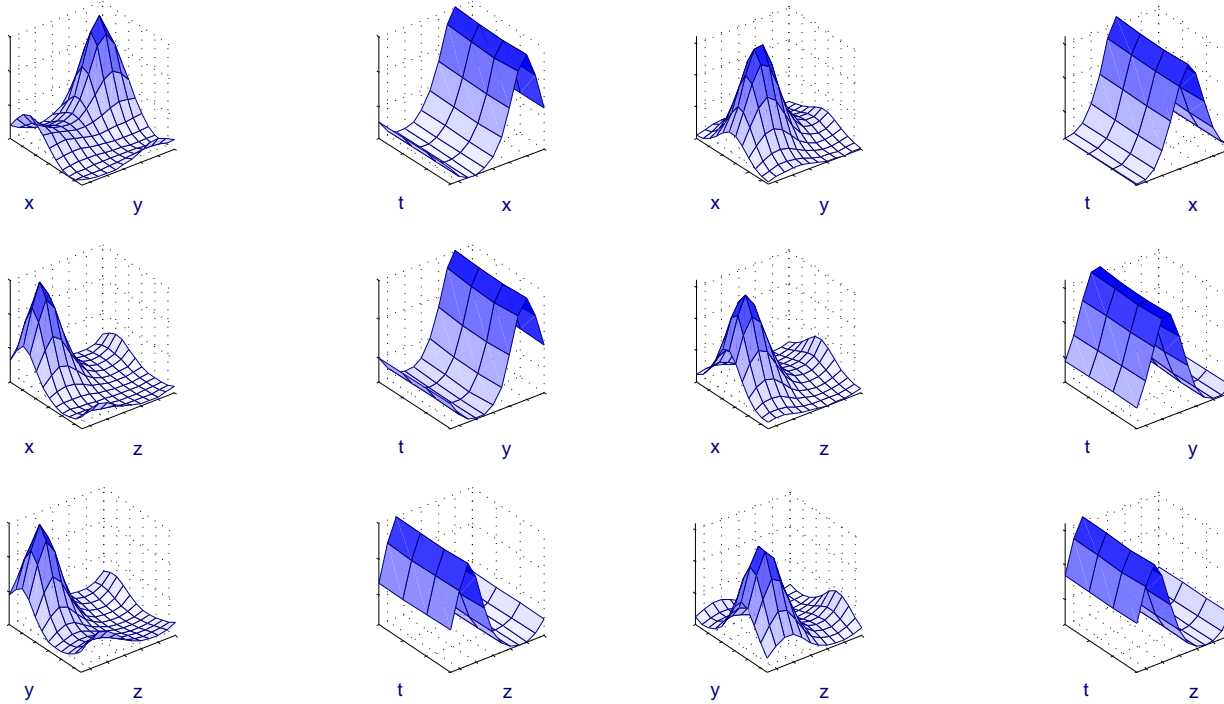


Figure 3: Jumping zero mode ( $\zeta = 0.1$  left and  $\zeta = 0.4$  right) of a static caloron with two well-separable constituents.



# No zero mode jumping in a non-static $|Q| = 1$ caloron on $12^3 \times 4$ :

cfg 157 phase 01 mode 1/1 with txyz=03 06 09 06

cfg 157 phase 04 mode 1/1 with txyz=03 06 09 07

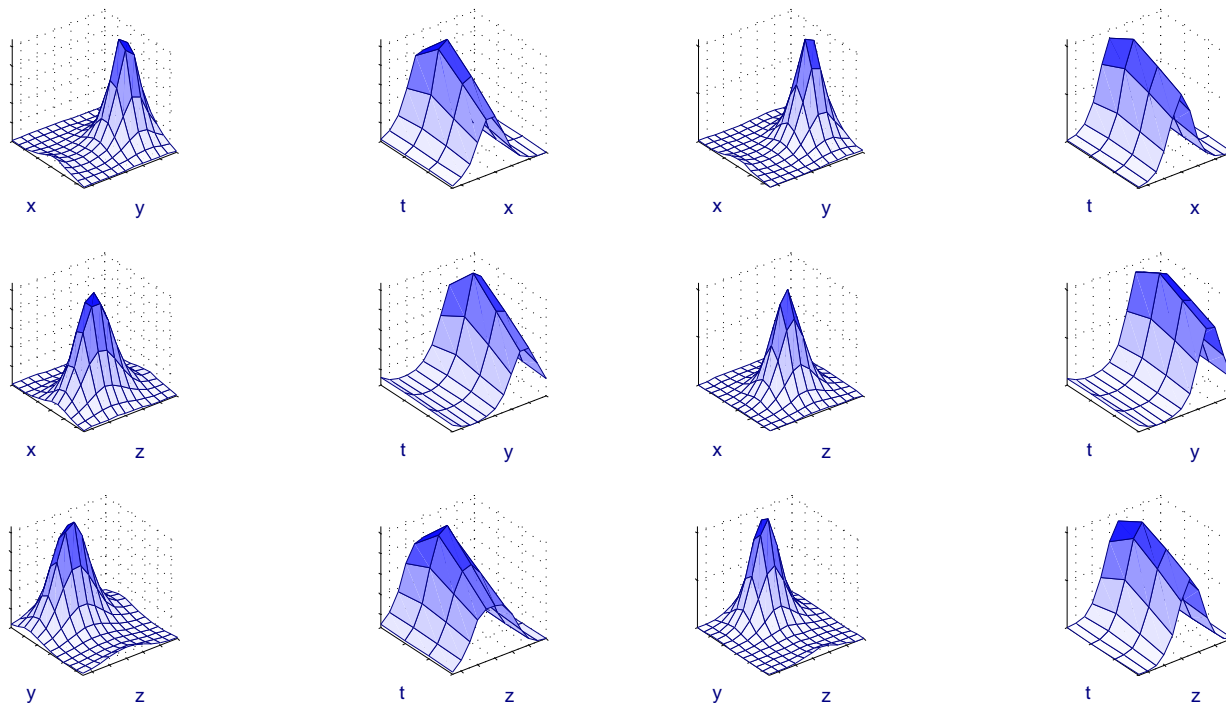


Figure 4: Zero mode not jumping ( $\zeta = 0.1$  left and  $\zeta = 0.4$  right) of a non-static caloron (close constituents).

A  $Q = 2$  caloron on a  $20^3 \times 4$  lattice

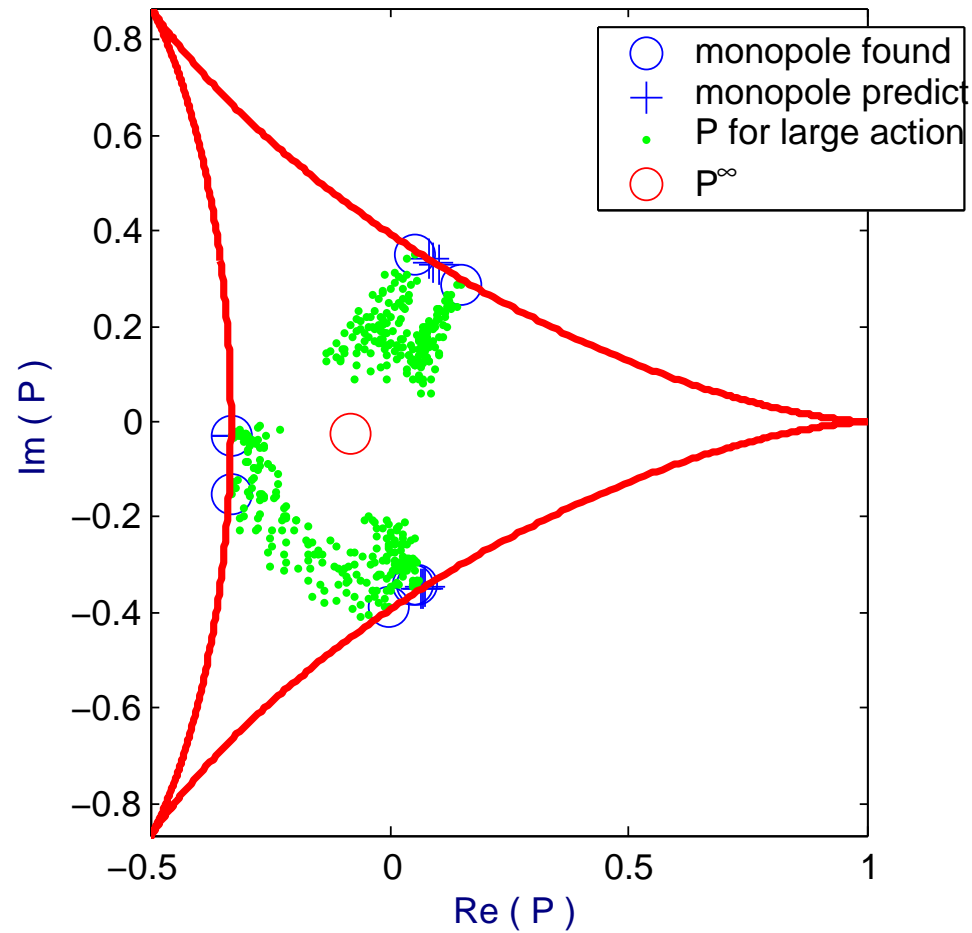
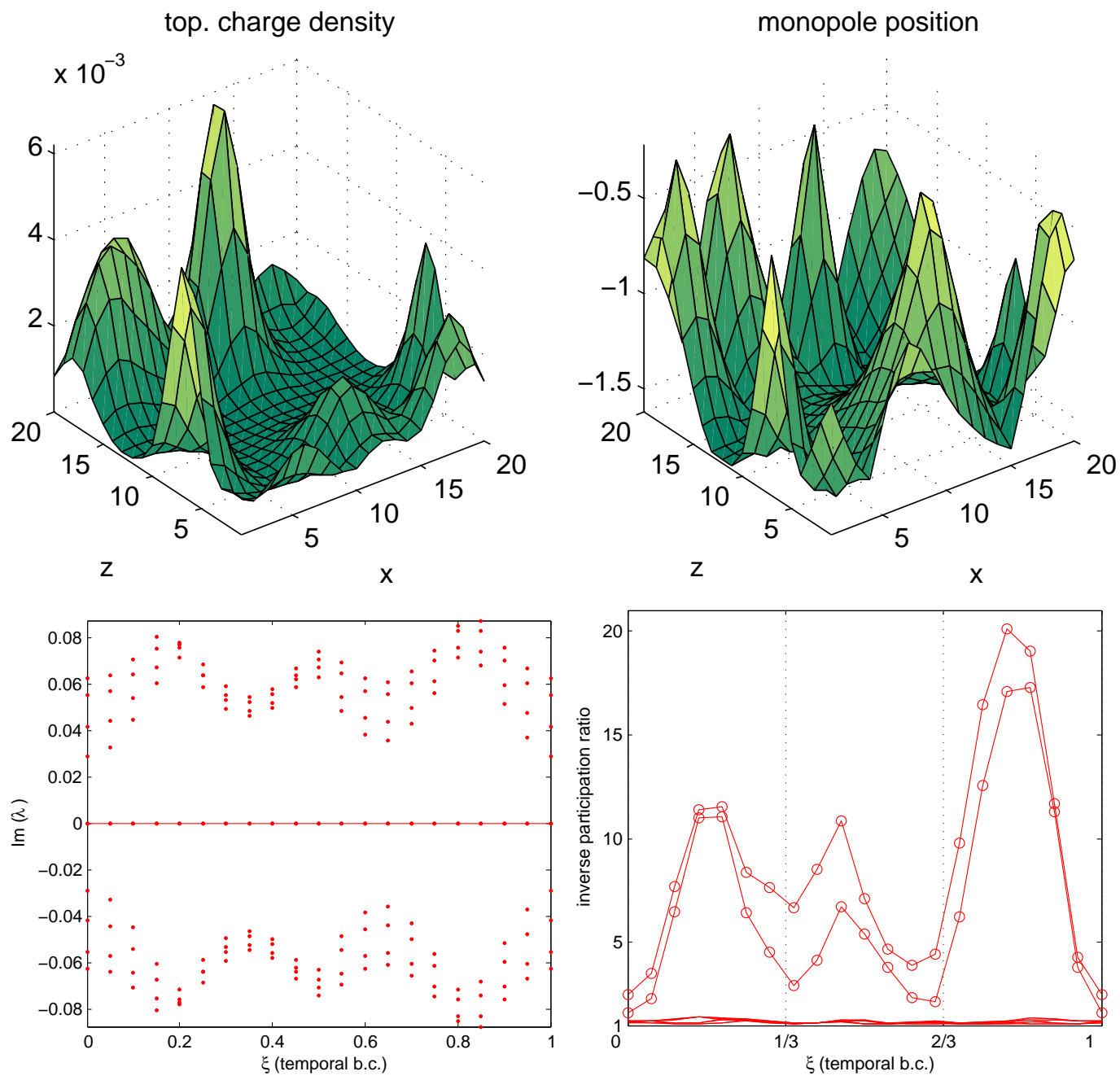


Figure 5:  $Q = 2$  caloron: Polyakov loop scatter plot at high action density.  
Notice the full number of monopole constituents.



**Figure 6:**  $Q=2$  caloron : Action density (upper left) and magnetic monopoles (upper right); spectral flow (bottom left) and IPR (bottom right) of the two zero modes.

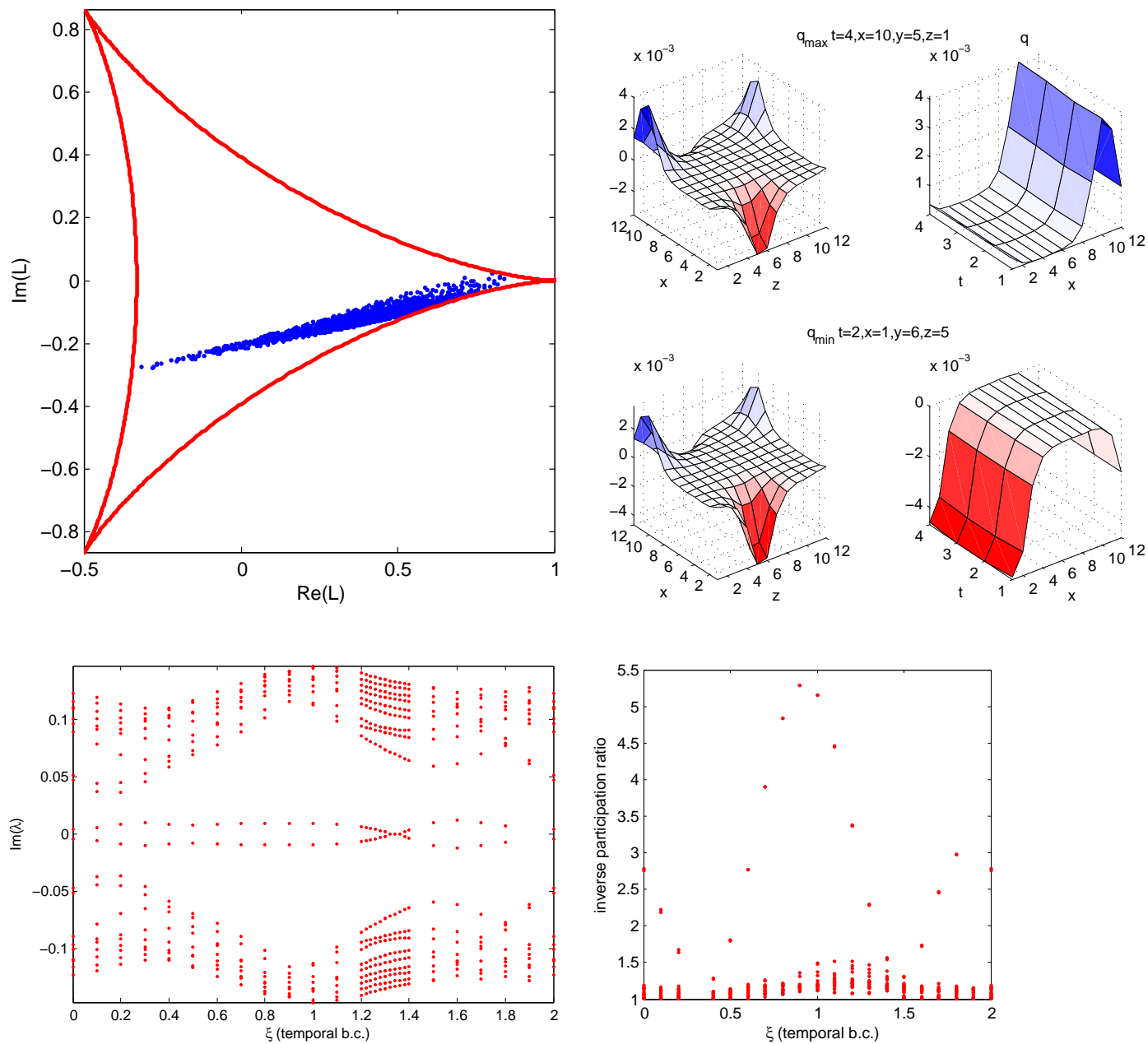


Figure 7: A  $Q = 0$  configuration on  $12^3 \times 4$  : a pair of static embedded SU(2) instanton/antiinstanton.

# Properties of cooled ensembles

Covering full moduli space in a finite volume,  
role of the "aspect ratio"  $L_t/L_s$

We have cooled Monte Carlo generated lattice configurations  
to the first classical plateau with

$|Q| = 1$ ,  $|Q| = 2$ ,  $|Q| = 3$  and  $|Q| = 4$  (and  $Q = 0$ )

$12^3 \times 4$  at  $\beta = 5.65$

ensemble A : 6000 configurations,

with cooling stopped for minimal violation of eq. of motion;

ensemble B : 9000 configurations,

with cooling stopped for maximal staticity;

ensemble C : 5000 configurations from ensemble B, violation of  
selfduality restricted to  $\delta_F < 0.1$

Other lattice sizes

$20^3 \times 4$  at  $\beta = 5.65$  (effect of expanded volume)

ensemble  $O(200)$  configurations

$12^3 \times 6$  (same  $\beta$ ) (effect of lower "temperature")

ensemble 3500 configurations, reduced 2500 configurations

$20^3 \times 6$  (same  $\beta$ ) (lower "temperature", expanded volume)

ensemble  $O(100)$  configurations

From the study of  $SU(2)$  calorons it was known :

lower "temperature"  $\rightarrow$  smaller distances between constituents,  
stronger overlap, more instanton-like for  $T \rightarrow 0$

"Recombination of dyons into calorons in  $SU(2)$  lattice fields at low temperatures", hep-lat/0402010

Classical property, does not reflect  $T$  of the hot sample !

## Distributions of non-staticity for $SU(2)$ calorons (PRD 69, 114505)

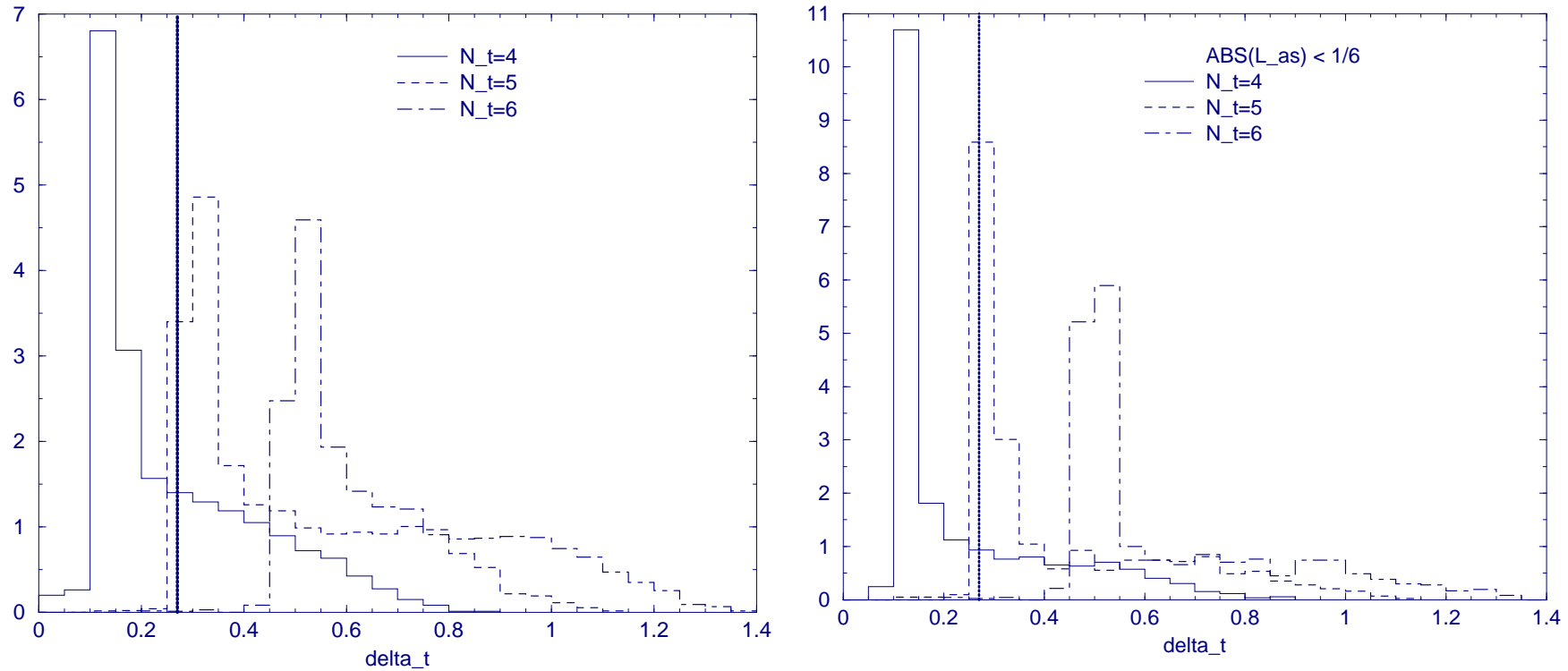


**Figure 8:** Getting more instanton-like at lower temperature. Histograms of non-staticity without cut (left) and with cut (right) restricting holonomy to  $L \approx 0$ . The vertical line marks the bifurcation into dyon constituents.

## Distributions of non-staticity for $SU(2)$ calorons (PRD 69, 114505)

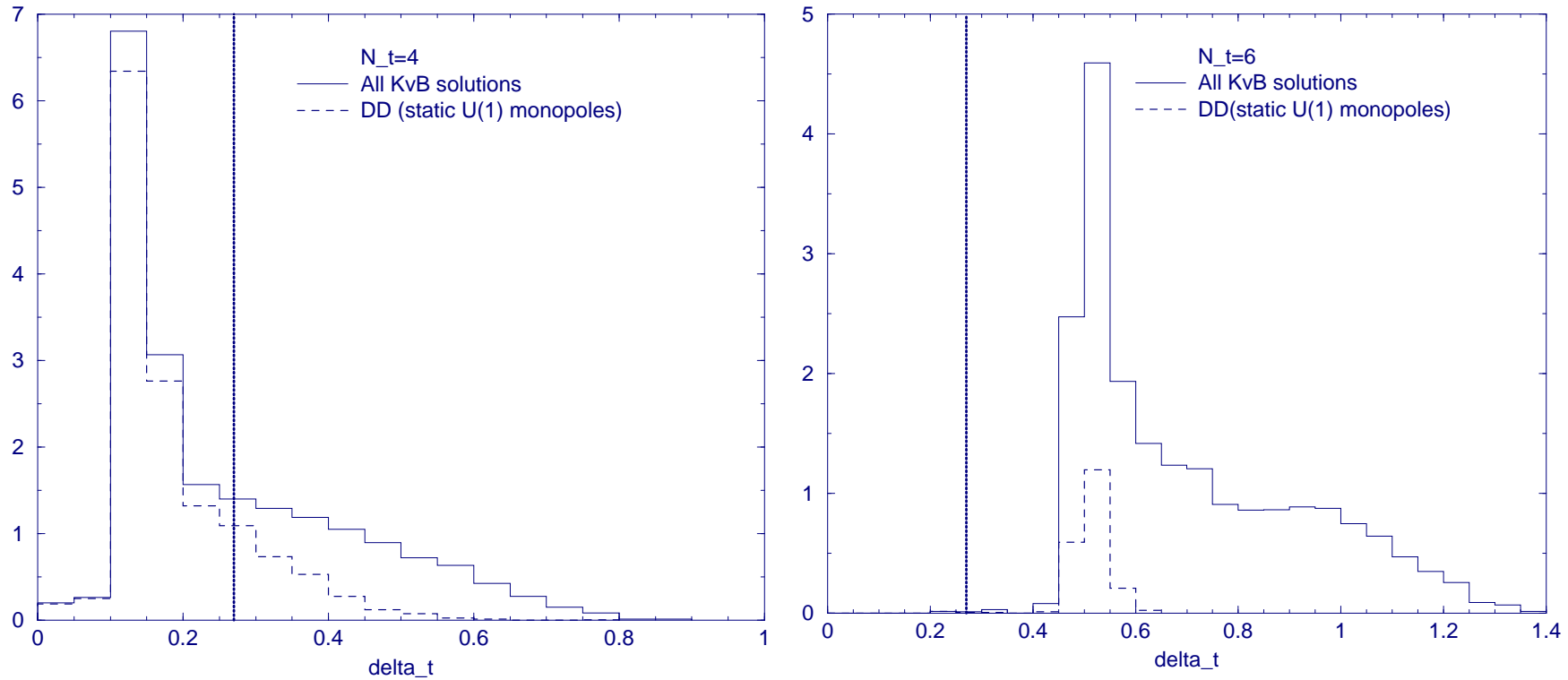


Figure 9: Histograms of the full sample compared with the subsample with static monopoles at high  $T$  (left) and lower  $T$  (right). The vertical line marks the bifurcation into dyon constituents.



## Distributions of non-staticity for $SU(3)$ calorons

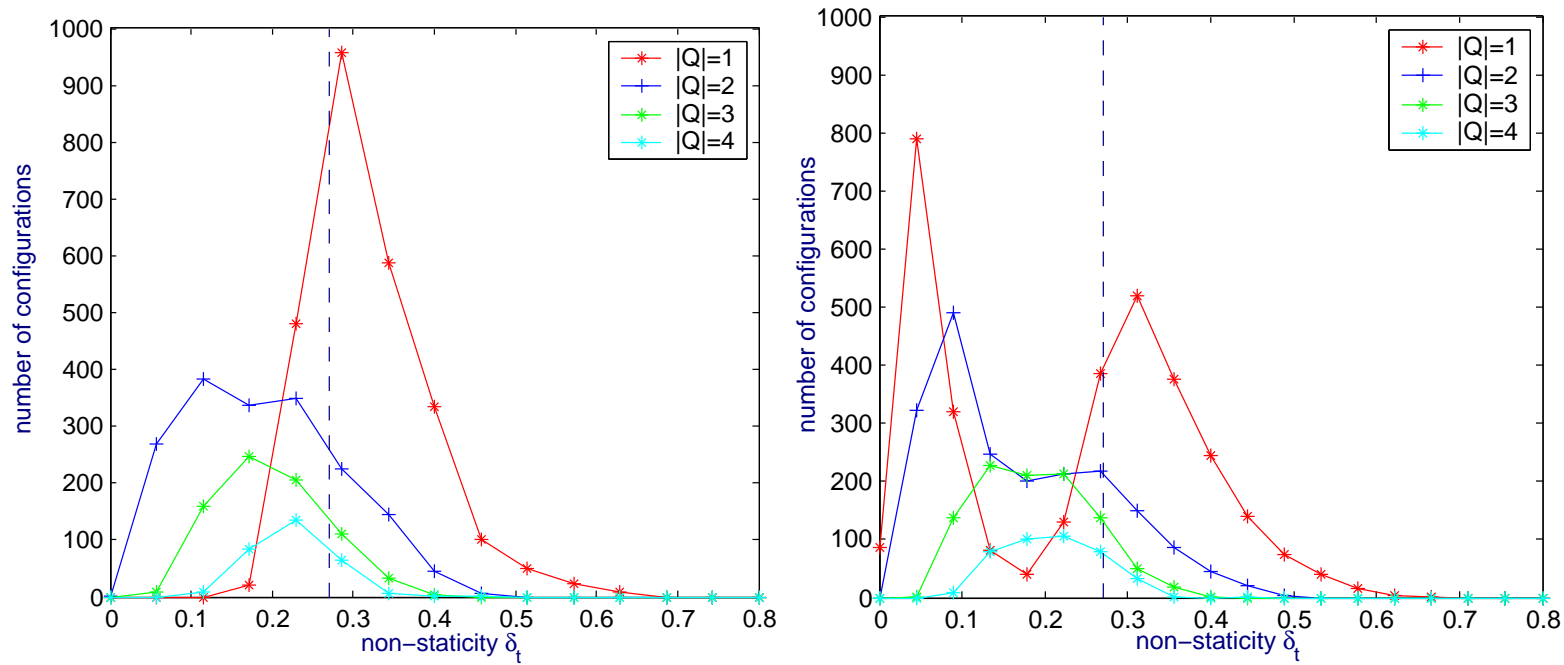


Figure 10: Distribution of non-staticity for various  $Q$ , for minimal violation of equations of motion (left) and for a combined stopping criterion (right). The vertical line marks the bifurcation of a caloron into constituents.

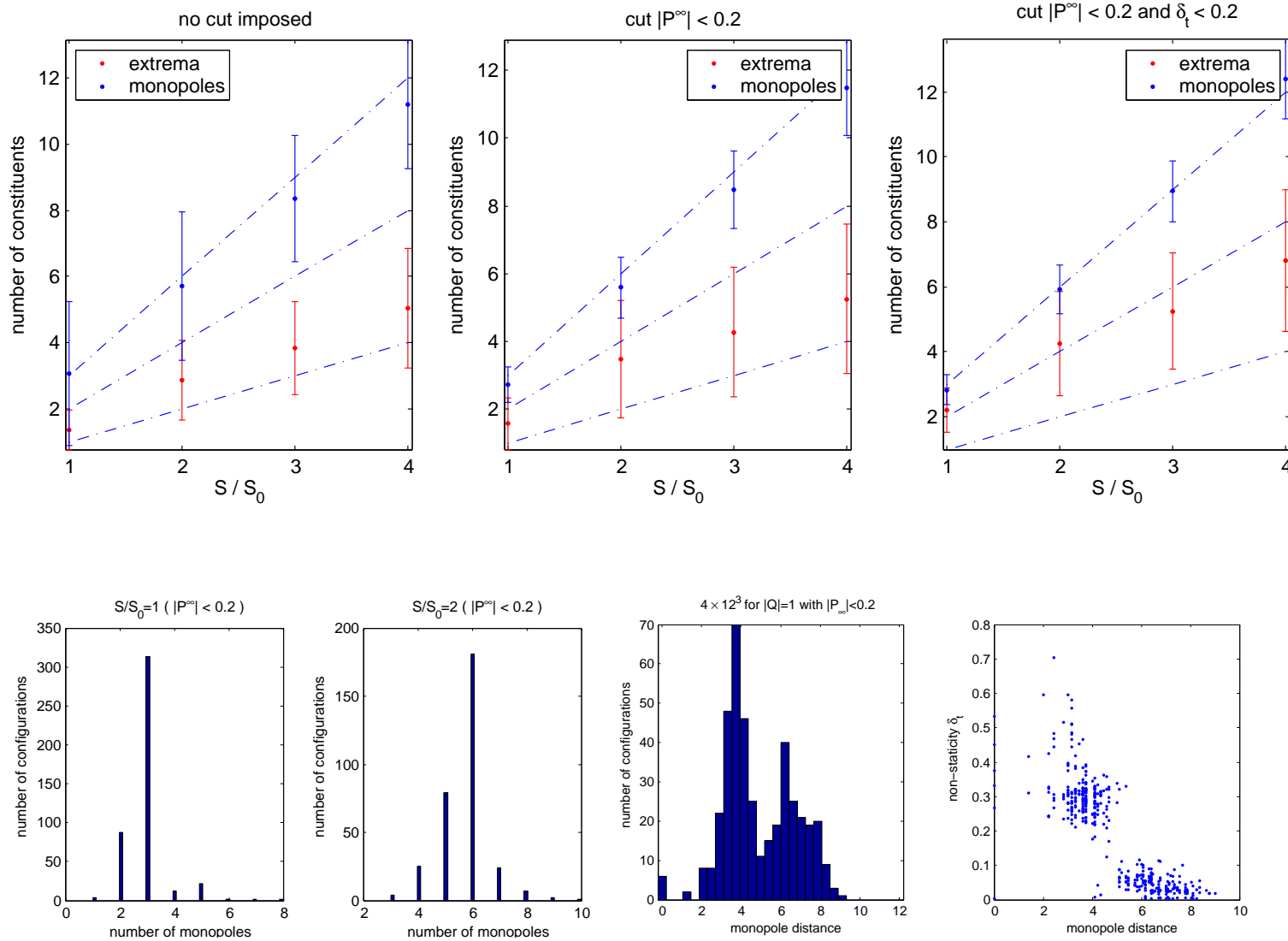


Figure 11: The number of monopoles and of discernible lumps versus  $|Q| = S/S_{inst}$  (upper row). Multiplicity of monopole constituents for  $|Q| = 1$  and  $|Q| = 2$  (bottom left). Distance between monopoles correlated with non-staticity (bottom right).

## Effect of bigger volume and lower temperature

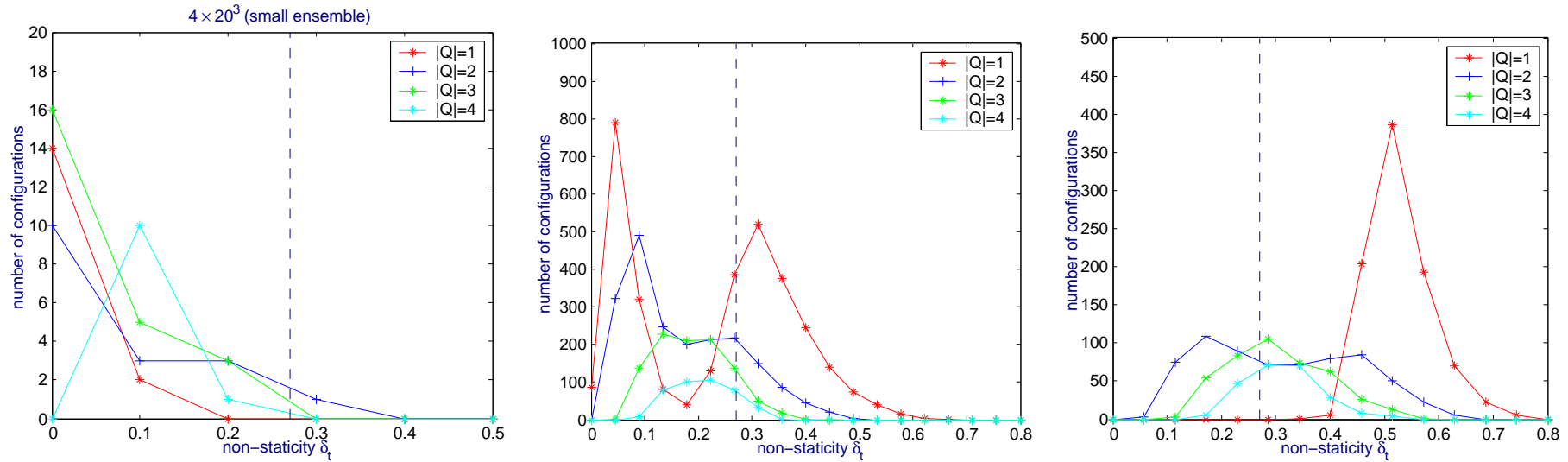


Figure 12: Distribution of non-staticity for various  $Q$ , compared to  $12^3 \times 4$  (middle), for larger volume (left) and for lower temperature (right).

# Summary & outlook

- Using cooling, we have systematically studied the characteristic features of  $SU(3)$  calorons at high temperature.
- At  $T \sim T_{dec}$  they resemble KvBLL calorons, although they are constructed in a finite volume.
- The monopole structure changes with lower temperature and/or larger volume.
- This study was restricted to classical configurations.
- In order to detect a caloron dissociation mechanism at the confinement transition we propose to use, in addition to the fermionic probes (Gattringer et al.), to study the magnetic charge content of topological clusters in (moderately APE smeared) equilibrium configurations.
- Work in this direction is in progress (so far for the  $SU(2)$  confinement transition).